Ultrafast measurement of optical-field statistics by dc-balanced homodyne detection

M. G. Raymer, J. Cooper,* and H. J. Carmichael

Department of Physics and Chemical Physics Institute, University of Oregon, Eugene, Oregon 97403

M. Beck

Department of Physics, Reed College, Portland, Oregon 97202

D. T. Smithey

Bend Research, 64550 Research Road, Bend, Oregon 97701

Received January 1, 1995; revised manuscript received April 21, 1995

The technique of dc-balanced, pulsed homodyne detection for the purpose of determining optical-field statistics on short time scales is analyzed theoretically. Such measurements provide photon-number and phase distributions associated with a repetitive signal light field in a short time window. Time- and space-varying signal and local-oscillator pulses are treated, thus generalizing earlier treatments of photoelectron difference statistics in homodyne detection. Experimental issues, such as the effects of imperfect detector balancing on (time-integrated) dc detection and the consequences of background noise caused by non-mode-matched parts of the multimode signal field, are analyzed. The Wigner, or joint, distribution for the two field-quadrature amplitudes during the sampling time window can be directly determined by tomographic inversion of the measured photoelectron distributions. It is pointed out that homodyne detection provides a new method for the simultaneous measurement of temporal and spectral information. Although the theory is generally formulated, with both signal and local-oscillator fields being quantized, emphasis is placed on the limit of a strong, coherent local-oscillator field, making semiclassical interpretation possible. © 1995 Optical Society of America

1. INTRODUCTION

Since balanced optical homodyne detection was developed by Yuen and Chan[1] and Abbas *et al.* in 1983,[2] it has been used widely in both continuous-wave[3] and pulsed-laser[4] applications for characterizing the quadrature-amplitude fluctuations of weak optical fields. Recently the measurement of the full probability distribution of the quadrature amplitudes was demonstrated,[5,6] generalizing earlier experiments that measured only the variance of the quadrature amplitudes. The distribution was measured by pulsed, balanced homodyne detection with integrating (dc) photodetectors, a technique that permits the statistical characterization of weak, repetitive optical fields on ultrafast time scales.[7,8] This technique detects optical field amplitudes in a particular spatial–temporal mode defined by a local-oscillator (LO) pulse. The LO pulse must be phase locked to the signal field and ideally would have a known spatial–temporal shape. Combined with the data processing method of tomographically reconstructing the joint (Wigner) distribution $W_S(x, y)$ for the two quadrature-field amplitudes x and y, the method is called optical homodyne tomography.[5,6] From the Wigner distribution one can obtain the probability distributions of optical intensity and phase relevant to a given spatial–temporal mode.[9] The technique can in principle have a quantum efficiency exceeding 99%, it operates at the shot-noise level, and it has been demonstrated to be capable of detecting a mean of less than one signal photon in a subpicosecond resolution time, after sufficient averaging.[7,9] The method has been applied to the time-resolved detection of pulsed squeezed light,[5,8] to light pulses after multiple scattering in a diffuse medium,[7] and to statistics of relaxation oscillations in a pulsed semiconductor diode laser.[10] Future applications may include time-resolving intensity fluctuations from light sources with short correlation times, such as superluminescent semiconductor laser diodes. It could also be used to observe the time dependence of spontaneous emission signals.

This paper provides a detailed theoretical analysis of the homodyne tomography method, which was summarized briefly in Ref. 6. We emphasize pulsed, balanced homodyne detection at zero frequency (dc) to model the recent experiments. Particular attention is given to experimental issues, such as effects of imperfect detector balancing on dc detection and the consequences of background noise caused by non-mode-matched parts of the multimode signal field, aspects that have not been examined in detail in previous discussions of homodyne detection.[11–18] We also make contact with recent theories of balanced homodyne detection that assume only one mode in the signal field.[19–24] The effect of optical losses on the reconstruction of the classical or quantum state from the homodyne distributions is discussed.[25] To reach the widest audience, we derive the results in a way that can be interpreted either semiclassically or quantum mechanically.

0740-3224/95/101801-12$06.00

The Wigner distribution plays a natural role in the quantum theory of homodyne detection, as its marginal distributions give directly the measured quadrature-amplitude statistics.[26] Because of this property, the Wigner distribution can be directly determined by tomographic inversion of the measured photoelectron distributions. For this reason it is emphasized here. In the case of a classical-like field (as from most lasers) the Wigner distribution can be simply interpreted as the joint distribution for the field quadrature amplitudes. In the case of a quantized field it is uniquely related to the quantum state (density matrix or wave function) of a spatial–temporal mode of the signal field. By reconstructing the Wigner distribution from the measurements, one determines the quantum state, which determines the signal's photon-number statistics and phase statistics, among other quantities.[6,9,27]

2. BALANCED HOMODYNE DETECTION

Balanced homodyne detection, shown in Fig. 1, has the advantage that it rejects intensity fluctuations of the LO field while measuring the signal quadrature-field amplitude in a particular spatial–temporal mode.[1,2] Such a mode is defined by the space–time form of the LO pulse.[12] In homodyne detection the signal and LO fields have spectra centered at the same, or nearly the same, optical frequency. The signal electric field $\hat{E}_S^{(+)}$ interferes with the LO field $\hat{E}_L^{(+)}$ at the lossless beam splitter to produce two output fields,[28–30]

$$\hat{E}_1^{(+)} = t_1\hat{E}_S^{(+)} + r_2\hat{E}_L^{(+)},$$
$$\hat{E}_2^{(+)} = r_1\hat{E}_S^{(+)} + t_2\hat{E}_L^{(+)}, \tag{2.1}$$

where unitarity of the transformation requires that the transmission and reflection coefficients satisfy $r_1t_2^* + t_1r_2^* = 0$. (In the case that the fields are quantum operators, this guarantees that the output fields commute.) For simplicity we assume the phase convention $t_1 = -t_2 = t$, $r_1 = r_2 = r$ and assume that t and r have values close to $(1/2)^{1/2}$, corresponding to a 50/50 beam splitter and thus to good balancing. Throughout this paper we assume linearly and copolarized fields.

The LO field is usually assumed to be a strong, pulsed coherent field from a laser. The fields hitting the photodiode detectors generate photoelectrons with probability (quantum efficiency) η, and the resulting current is integrated by low-noise charge-sensitive amplifiers.[31,32] This provides the dc detection and differs from the often-used method of using radio-frequency spectral analysis of the current to study noise at higher frequencies.[2–4] The values of the integrated photocurrents are recorded with analog-to-digital converters to give the numbers of photoelectrons n_1 and n_2 per pulse. As seen below, the difference of these numbers is proportional to the chosen electric-field quadrature amplitude of the signal, time averaged over the window defined by the duration of the LO pulse.

We will assume that the photodetectors respond to the incident photon flux. This approach is slightly different from the usual Glauber–Kelly-Kleiner formulation in which the observed photoelectron current is in terms of the electromagnetic energy density at the detector.[33,34] The approach used here is considered to be more appropriate for broadband fields in the case that the detector's quantum efficiency is frequency independent, i.e., the detector is a photoemissive rather than an energy-flux detector.[11–14,17,35,36] The free-space energy density in Gaussian units is $(1/2\pi)\hat{E}_i^{(-)}\hat{E}_i^{(+)}$, where the positive-frequency part of the electric field (operator) can be represented as

$$\hat{E}_S^{(+)}(\mathbf{r}, t) = i\sum_{j,l}\int \mathrm{d}k_z\sqrt{\hbar\omega_j/2\pi D^2}\,\hat{a}_{jl}(k_z) \times \exp[-i\omega_{jl}(k_z)t + i\mathbf{k}_{jl}\cdot\mathbf{r}]. \tag{2.2}$$

The longitudinal propagation constant k_z has been treated as a continuous variable to allow for pulse propagation in the z direction, and the transverse part has been treated discretely, with the propagation vector given by $\mathbf{k}_{jl} = \mathbf{z}k_z + (\mathbf{y}n_{yl} + \mathbf{x}n_{xj})2\pi/D$, with n_{yl} and n_{xj} integers and D the transverse quantization dimension (width and height of detector). In the classical theory $\hat{a}_{jl}(k_z)$ are complex mode amplitudes. In the quantum theory they are annihilation operators obeying the commutator

$$[\hat{a}_{jl}(k_z), \hat{a}_{nm}{}^{\dagger}(k_z{}')] = \delta_{jn}\delta_{lm}2\pi\delta(k_z - k_z{}'). \tag{2.3}$$

(Generally a caret over a variable indicates an operator.) In the paraxial approximation the frequencies are given by[37]

$$\omega_{jl}(k_z) \cong c[k_z + (n_{yl}{}^2 + n_{xj}{}^2)(2\pi/D)^2/2K], \tag{2.4}$$

where K is an average value of k_z. This is valid as long as the beam propagates primarily in the z direction and has a bandwidth much less than the optical frequency.

A photon-flux amplitude $\hat{\Phi}_S^{(+)}(\mathbf{r}, t)$ can be defined for the signal as[11–14,17,35,36]

$$\hat{\Phi}_S^{(+)}(\mathbf{r}, t) = i\,\frac{c^{1/2}}{2\pi D}\sum_{j,l}\int_0^{\infty}\mathrm{d}k_z\hat{a}_{jl}(k_z) \times \exp[-i\omega_{jl}(k_z)t + i\mathbf{k}_{jl}\cdot\mathbf{r}], \tag{2.5}$$

where only waves traveling in the $+z$ direction are included, and similarly for the LO field. The photon fluxes

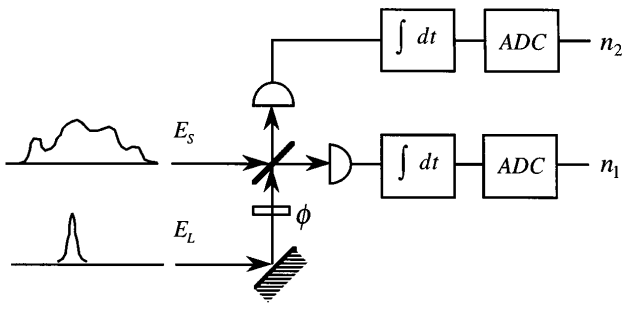

Fig. 1. A signal pulse field $\hat{E}_S$ interferes with a shorter LO pulse $\hat{E}_L$ at a 50/50 beam splitter. The LO phase ϕ determines which quadrature amplitude of the signal is detected. The superposed fields are detected with high-efficiency photodiodes having response times much longer than the pulse durations. The photocurrents are integrated and sampled by analog-to-digital converters (ADC's), to yield pulse photoelectron numbers n_1 and n_2.

(photons/s) of the output fields ($i = 1, 2$) at the detector faces are then represented by

$$\hat{I}_i(t) = \int_{\mathrm{Det}} \mathrm{d}^2 s \hat{\Phi}_i^{(-)}(\mathbf{s}, t)\hat{\Phi}_i^{(+)}(\mathbf{s}, t)\,, \tag{2.6}$$

integrated over the detectors' faces, where $\mathbf{s}$ denotes the transverse variables. In classical theory the photon is simply a convenient unit of light energy. It is assumed that the quantities $\hat{\Phi}^{(+)}(\mathbf{r}, t)$ obey the same transformations at the beam splitter as do the fields in Eq. (2.1). The photon number contained in a time interval $(0, T)$ at each detector is represented by $\hat{N}_i = \int_0^T \hat{I}_i \mathrm{d}t$. The interval duration T is assumed to be somewhat longer than the duration of the signal and LO pulses, so all the energy of each is detected. The electronic system, including the detector and the amplifiers used to process the photocurrent, has been assumed to act as a low-pass filter with an integration time (inverse bandwidth) much larger than T. The difference-photon number contained in a time interval $(0, T)$ is represented by

$$\hat{N}_{12} = \hat{N}_1 - \hat{N}_2 = \int_0^T (\hat{I}_1 - \hat{I}_2)\mathrm{d}t\,, \tag{2.7}$$

and the total photon number is

$$\hat{N}_T = \hat{N}_1 + \hat{N}_2 = \int_0^T (\hat{I}_1 + \hat{I}_2)\mathrm{d}t\,. \tag{2.8}$$

In the case of perfect balancing ($r = t$) the difference number is given in terms of the input fields by

$$\hat{N}_{12} = \int_0^T \mathrm{d}t \int_{\mathrm{Det}} \mathrm{d}^2 s(\hat{\Phi}_L^{(-)}\hat{\Phi}_S^{(+)} + \hat{\Phi}_S^{(-)}\hat{\Phi}_L^{(+)})\,. \tag{2.9}$$

The effects of imperfect balancing are considered below.

Note, as mentioned above, that this implementation of balanced homodyne detection is somewhat different from the customary case, in which a radio-frequency spectrum analyzer is used to detect the oscillations of photocurrent at some frequency other than zero. This is usually done for the purpose of reducing electronic noise. Recently detection at zero frequency (dc) was demonstrated,[5,6] and this is the case that we analyze. The non-dc case can easily be analyzed by insertion into Eqs. (2.7) and (2.8) of a time-domain filter function centered at some nonzero frequency.[14,15,18]

At this stage the LO field (which may be considered quantized or not) will be specialized to the case in which it factorizes at each detector face into a transverse spatial part $u_L(\mathbf{s})$ and a temporal part $f_L(t)$. This can be accomplished experimentally in a given plane, where the detector is located, whereas at any other plane the field will in general not so factorize. This separation assumes that the LO is excited in a single spatial-temporal mode,[11–13,37,38,39] which is the same for each laser pulse. It does not, however, require this mode to be a chirp-free, transform-limited pulse: it may have a complicated time dependence of phase or amplitude. [In the case that the LO field does not factorize in the detector plane it can be expanded as a sum of factorized fields (spatial-temporal modes). The homodyne statistics can be analyzed in terms of these modes.[40]] Thus we have at the detectors

$$\hat{\Phi}_L^{(+)} = i\hat{a}_L f_L(t)u_L(\mathbf{s})\,, \tag{2.10}$$

where the functions are normalized as

$$\int_0^T |f_L(t)|^2 \mathrm{d}t = 1\,, \qquad \int_{\mathrm{Det}} |u_L(\mathbf{s})|^2 \mathrm{d}^2 s = 1\,, \tag{2.11}$$

so that $\hat{a}_L$ is the complex amplitude (or annihilation operator for photons) for the LO spatial–temporal mode, which is defined by the function $u_L(\mathbf{s})f_L(t)$. In quantum theory $\hat{a}_L$ satisfies $[\hat{a}_L, \hat{a}_L{}^\dagger] = 1$. The function $u_L(\mathbf{s})f_L(t)$ may be regarded as one member of a complete orthonormal basis of functions that can be built up from $u_L(\mathbf{s})f_L(t)$ by the standard Schmidt procedure.[41] In principle it would be possible to measure the quadrature statistics in a complete set of LO modes and thereby build up a detailed picture of the temporal and spatial structure of the signal pulse. In this paper, however, we concentrate on measuring the statistics in only one of these LO modes, which we may assume to be fully known through a technique such as frequency-resolved optical gating.[42]

Using Eq. (2.10) in Eq. (2.9) yields for the total photon number striking the detectors

$$\hat{N}_T = \hat{a}_L{}^\dagger \hat{a}_L + \hat{N}_S\,, \tag{2.12}$$

where the signal photon number is

$$\hat{N}_S = \int_0^T \mathrm{d}t \int_{\mathrm{Det}} \mathrm{d}^2 s \hat{\Phi}_S^{(-)}(\mathbf{s}, t)\hat{\Phi}_S^{(+)}(\mathbf{s}, t)\,. \tag{2.13}$$

The difference number is given by

$$\hat{N}_{12} = \hat{a}\hat{a}_L{}^\dagger + \hat{a}^\dagger \hat{a}_L\,, \tag{2.14}$$

where

$$\hat{a} = -i \int_0^T \mathrm{d}t \int_{\mathrm{Det}} \mathrm{d}^2 s f_L{}^*(t)u_L{}^*(\mathbf{s})\hat{\Phi}_S^{(+)}(\mathbf{s}, t)\,. \tag{2.15}$$

Classically the amplitude $\hat{a}$ is the signal field sampled by the space–time window function defined by the LO. In quantum theory the operator $\hat{a}$ commutes with $\hat{a}_L{}^\dagger$ and also satisfies $[\hat{a}, \hat{a}^\dagger] = 1$ in the paraxial approximation, which is typically valid in homodyne detection experiments. (This is proved in Appendix A.) Therefore the amplitude $\hat{a}$ can be interpreted as the annihilation operator for the detected part of the signal field, that is, that part corresponding to, or mode matched to, the spatial-temporal mode $u_L(\mathbf{s})f_L(t)$ defined by the LO.

Because $\hat{a}$ is the complex amplitude for the detected part of the signal field, we can represent it by a phasor with real and imaginary parts given by $\hat{x} = (\hat{a} + \hat{a}^\dagger)/2^{1/2}$ and $\hat{y} = (\hat{a} - \hat{a}^\dagger)/i2^{1/2}$. (Here the dagger represents complex conjugation, or the Hermitian adjoint in the quantum case.) These two variables are called quadrature amplitudes for the detected mode. In the quantum case $\hat{x}$ and $\hat{y}$ are Hermitian operators that obey the commutator $[\hat{x}, \hat{y}] = i$ for a pair of conjugate variables. They are mathematically analogous to the position and momentum operators for a quantized harmonic oscillator (with $\hbar = 1$).

If the LO field is coherent and strong, and treated classically, with amplitude $\hat{a}_L$ in Eq. (2.14) replaced by $\alpha_L = |\alpha_L|\exp(i\phi)$, then the difference number becomes

$$\hat{N}_{12} = |\alpha_L|[\hat{a}\exp(-i\phi) + \hat{a}^\dagger \exp(i\phi)]. \tag{2.16}$$

Thus for the LO phase equal to zero the balanced homodyne detector measures the real quadrature $\hat{x}$, whereas for the LO phase equal to $\pi/2$ it measures the imaginary quadrature $\hat{y}$. We define the generalized quadrature amplitude

$$\hat{x}_\phi = \hat{N}_{12}/(|\alpha_L|2^{1/2}) = [\hat{a}\exp(-i\phi) + \hat{a}^\dagger \exp(i\phi)]/2^{1/2}. \tag{2.17}$$

This is the quantity measured by this scheme. A complementary variable can be defined by

$$\hat{y}_\phi = [\hat{a}\exp(-i\phi) - \hat{a}^\dagger \exp(i\phi)]/i2^{1/2}. \tag{2.18}$$

These variables may be considered as resulting from a rotation in the x–y phase space of the original variables, i.e.,

$$\begin{pmatrix} \hat{x}_\phi \\ \hat{y}_\phi \end{pmatrix} = \begin{pmatrix} \cos\phi & \sin\phi \\ -\sin\phi & \cos\phi \end{pmatrix} \begin{pmatrix} \hat{x} \\ \hat{y} \end{pmatrix}. \tag{2.19}$$

In quantum theory the variables $\hat{x}_\phi$ and $\hat{y}_\phi$ do not commute and so cannot be measured jointly with arbitrarily high precision. Their standard deviations obey the uncertainty relation

$$\Delta\hat{x}_\phi \Delta\hat{y}_\phi \geq 1/2. \tag{2.20}$$

For coherent states both standard deviations equal $1/2^{1/2}$, whereas for squeezed states one, but not both, of these standard deviations can be less than this value.[43]

3. JOINT PHOTOELECTRON COUNTING DISTRIBUTION

The photoelectron counting distribution for the four-port homodyne detector shown in Fig. 1 is derived here. We follow, but generalize, recent single-mode theories of balanced homodyne detection in which the LO is treated quantum mechanically.[19,22,23] A wideband treatment has also been given by Collett *et al.*[21]

According to the theory of photoelectron detection the joint probability to observe n_1 photoelectrons in detector 1 and n_2 photoelectrons in detector 2 is given by[33,34]

$$P_{12}(n_1, n_2) = \left\langle : \frac{\exp(-\eta\hat{N}_1)(\eta\hat{N}_1)^{n_1}}{n_1!} \frac{\exp(-\eta\hat{N}_2)(\eta\hat{N}_2)^{n_2}}{n_2!} : \right\rangle_{S,L}, \tag{3.1}$$

where in the quantum case the angle brackets and double dots indicate a normal-ordered quantum expectation value over both signal and LO modes.[44,45] In the classical case the angle brackets simply represent an ensemble average over the random processes that describe the fluctuations of the signal and LO fields.[46,47] Note that we are using the photon-flux amplitudes $\hat{\Phi}_1^{(+)}$ and $\hat{\Phi}_2^{(+)}$ rather than the electric fields in Eq. (3.1). The quantum efficiency of the photodetectors is denoted η and lies between 0 and 1.

The probability to observe a difference photoelectron number $n_{12} = n_1 - n_2$ is given by

$$P(n_{12}) = \sum_{n_2} P_{12}(n_2 + n_{12}, n_2). \tag{3.2}$$

When we substitute Eq. (3.1) into Eq. (3.2) and use the fact that $\hat{N}_1$ and $\hat{N}_2$ commute, the summation leads to

$$P(n_{12}) = \left\langle : \exp[-\eta(\hat{N}_1 + \hat{N}_2)](\hat{N}_2/\hat{N}_1)^{n_{12}/2} \times I_{|n_{12}|}[2\eta(\hat{N}_1\hat{N}_2)^{1/2}] : \right\rangle_{S,L}, \tag{3.3}$$

where $I_n(x)$ is the modified Bessel function of nth order. This general result for the joint photoelectron probability was previously obtained in the case of single-mode fields[22,23] or in the case of multimode, coherent-state fields.[21] Our derivation generalizes the earlier ones in that it incorporates multimode, pulsed signal and LO fields in arbitrary states.

It is important to ask to what extent the multimode nature of the signal limits or degrades the information that can be obtained about the mode-matched part of the signal. By multimode it is meant that the signal cannot generally be written in a form analogous to Eq. (2.10). To address this it is useful to define a non-mode-matched, or background, part $\hat{\Phi}_B^{(+)}$ of the signal field by subtracting off the mode-matched part, using Eq. (2.15):

$$\hat{\Phi}_B^{(+)}(\mathbf{s}, t) = \hat{\Phi}_S^{(+)}(\mathbf{s}, t) - i\hat{a}f_L(t)u_L(\mathbf{s}) = \int_0^T dt' \int_{\text{Det}} d^2s' P_B(t, t', \mathbf{s}, \mathbf{s}')\hat{\Phi}_S^{(+)}(\mathbf{s}', t'), \tag{3.4}$$

where P_B is a projector onto the nonmatched modes:

$$P_B(t, t', \mathbf{s}, \mathbf{s}') = \delta(t - t')\delta^2(\mathbf{s} - \mathbf{s}') - f_L(t)u_L(\mathbf{s})f_L{}^*(t')u_L{}^*(\mathbf{s}'). \tag{3.5}$$

The number of photons in the non-mode-matched part of the signal is given by

$$\hat{N}_B = \int_0^T dt \int_{\text{Det}} d^2s \hat{\Phi}_B^{(-)}(\mathbf{s}, t)\hat{\Phi}_B^{(+)}(\mathbf{s}, t). \tag{3.6}$$

The number of signal photons in Eq. (2.13) may now be reexpressed exactly in terms of the single-mode amplitude and the nonmatched part as

$$\hat{N}_S = \hat{a}^\dagger\hat{a} + \hat{N}_B, \tag{3.7}$$

and the numbers of photons hitting each detector may be rewritten as

$$\hat{N}_1 = \left(\frac{\hat{a}_L{}^\dagger + \hat{a}^\dagger}{\sqrt{2}}\right)\left(\frac{\hat{a}_L + \hat{a}}{\sqrt{2}}\right) + \frac{\hat{N}_B}{2},$$
$$\hat{N}_2 = \left(\frac{\hat{a}_L{}^\dagger - \hat{a}^\dagger}{\sqrt{2}}\right)\left(\frac{\hat{a}_L - \hat{a}}{\sqrt{2}}\right) + \frac{\hat{N}_B}{2}. \tag{3.8}$$

These equations represent the fact that the LO and mode-matched signals interfere at the beam splitter, whereas the nonmatched signal simply splits 50/50.

The expression in Eq. (3.3) with $\hat{N}_1$ and $\hat{N}_2$ given by Eqs. (3.8) is a main result of this paper and permits the evaluation of difference-photon number statistics for arbitrary states of the multimode signal field and the single-mode LO field. It generalizes previous single-mode results ($\hat{N}_B = 0$)[22,23] as well as multimode, coherent-state results.[21] It provides a method to find the effects on the photoelectron statistics of the nonmatched part. Generally speaking, the nonmatched part will contribute extra shot noise to the measurement and broaden the measured distributions. Often the LO can be considered very intense, in that it dominates the shot noise; however, if the signal field is of much longer duration than the LO then the signal may dominate, on integration, even though its peak intensity is low.

The form of the distribution inside the angle brackets in Eq. (3.3) is known in classical statistics to be that for the difference of two variables, each obeying Poisson distributions. This provides a simple understanding of Eq. (3.3): it is the distribution resulting from two Poisson distributions, each resulting from a coherent state, averaged over the possible amplitudes of the fields, which may represent noncoherent states. The operator nature of the field allows the distribution of difference number in Eq. (3.3) to be narrower than the shot-noise level (defined below) for the same mean numbers of photons in each beam. The shape of the difference distribution in the macroscopic regime has been measured in twin-photon-beam experiments using parametric amplification, and narrowing to below the shot-noise level has been observed.[31,48] The sub-shot-noise-level width indicates a breakdown of the semiclassical interpretation of detector theory, in which incident fields are assumed to be in mixtures of coherent states (i.e., to have a positive-definite Glauber–Sudarshan P distribution).

4. INTENSE, COHERENT LOCAL OSCILLATOR

Our interest here is in analyzing detection of multimode signal fields rather than in studying the effects of weak, quantized LO fields, which have been discussed elsewhere.[22,23] So we will hereafter consider the LO field to be in a coherent state $|\alpha_L\rangle$ of the single spatial-temporal mode $u_L(\mathbf{s})f_L(t)$ such that $\hat{a}_L|\alpha_L\rangle = \alpha_L|\alpha_L\rangle$. Then, when evaluating Eq. (3.3), we replace the operator $\hat{a}_L$ [which enters by means of Eqs. (3.8)] by the complex variable $\alpha_L = |\alpha_L|\exp(i\phi)$, as an exact consequence of the normal ordering. Then we can study fluctuations of the LO field simply by averaging the distribution over an ensemble of α_L values:

$$P(n_{12}) = \int P(n_{12};\,\alpha_L)P_L(\alpha_L)\mathrm{d}^2\alpha_L\,, \tag{4.1}$$

where $P_L(\alpha_L)$ is a classical distribution function (Glauber P distribution[33,49,50]) for the complex LO amplitude and the distribution for a given α_L is

$$P(n_{12};\,\alpha_L) = \langle{:}\,\exp[-\eta(\hat{N}_1+\hat{N}_2)](\hat{N}_2/\hat{N}_1)^{n_{12}/2} \times I_{|n_{12}|}[2\eta(\hat{N}_1\hat{N}_2)^{1/2}]\,{:}\rangle_S\,. \tag{4.2}$$

The quantum expectation value is now over only the multimode signal field, denoted S, i.e., $\langle\ldots\rangle_S = \mathrm{Tr}(\hat{\rho}_S\ldots)$, where $\hat{\rho}_S$ is the density operator for the signal modes.[51] Note that, even though the LO may be instantaneously much more intense than the signal during the LO pulse, the total energy in the signal pulse may be greater than that in the LO pulse if the signal has much greater duration. In this case it is not accurate to neglect the nonmatched signal in Eqs. (3.8) when calculating the photoelectron statistics of the mode-matched part.

If the LO is strong in the sense of having many photons per pulse, then n_1 and n_2 are much greater than unity, and Eq. (4.2) can be well approximated by a Gaussian function[52]

$$P(n_{12};\,\alpha_L) = \left\langle{:}\,\frac{\exp[-(n_{12}-\eta\hat{N}_{12})^2/2\eta\hat{N}_T]}{[\pi 2\eta\hat{N}_T]^{1/2}}\,{:}\right\rangle_S\,, \tag{4.3}$$

where the difference number is here given by Eq. (2.16) and the total number of photons hitting both detectors is

$$\hat{N}_T = |\alpha_L|^2 + \hat{a}^\dagger\hat{a} + \hat{N}_B\,. \tag{4.4}$$

The total number of photons sets the scale for the shot-noise level.

As an important example, consider the case that the signal field is in a multimode coherent state $|\{\alpha_{jl}\}\rangle$, such that the $\alpha_{jl}(k_z)$ are eigenvalues of the $\hat{a}_{jl}(k_z)$ in Eq. (2.2). This leads to $\hat{\Phi}_S^{(+)}(\mathbf{s},t)|\{\alpha_{jl}\}\rangle = \hat{\Phi}_S^{(+)}(\mathbf{s},t)|\{\alpha_{jl}\}\rangle$, which means that the operator $\hat{\Phi}_S^{(+)}(\mathbf{s},t)$ appearing in Eq. (3.3) through Eqs. (3.8) and (2.15) is replaced by the complex amplitude $\Phi_S^{(+)}(\mathbf{s},t)$ given by

$$\Phi_S^{(+)}(\mathbf{r},t) = i\frac{c^{1/2}}{2\pi D}\sum_{j,l}\int_0^\infty \mathrm{d}k_z\,\alpha_{jl}(k_z) \times\exp[-i\omega_{jl}(k_z)t + i\mathbf{k}_j\cdot\mathbf{r}]\,. \tag{4.5}$$

Then the mode-matched signal amplitude $\hat{a}$ defined in Eq. (2.15) generates the eignenvalue equation $\hat{a}|\{\alpha_{jl}\}\rangle = \alpha|\{\alpha_{jl}\}\rangle$, where the classical detected amplitude is

$$\alpha = -i\int_0^T \mathrm{d}t\int_{\mathrm{Det}}\mathrm{d}^2s f_L{}^*(t)u_L{}^*(\mathbf{s})\Phi_S^{(+)}(\mathbf{s},t)\,. \tag{4.6}$$

The mean number of photons in the signal field is

$$\overline{N}_S = \langle\hat{N}_S\rangle = \int_0^T \mathrm{d}t\int_{\mathrm{Det}}\mathrm{d}^2s\,\Phi_S^{(-)}(\mathbf{s},t)\Phi_S^{(+)}(\mathbf{s},t) = |\alpha|^2 + \overline{N}_B\,, \tag{4.7a}$$

where the mean nonmatched signal is

$$\overline{N}_B = \int_0^T \mathrm{d}t\int_{\mathrm{Det}}\mathrm{d}^2s\,\Phi_B^{(-)}(\mathbf{s},t)\Phi_B^{(+)}(\mathbf{s},t) \tag{4.7b}$$

and $\Phi_B^{(+)}$ is given by an expression analogous to Eq. (3.4). Note that $\overline{N}_B$ is a constant if the non-mode-matched signal is in a coherent state or in a wideband thermal state with a coherence time much less than T. Also note that $\overline{N}_S$ is not equal to $|\alpha|^2$ unless the signal field is excited only in the same spatial-temporal mode as the LO, i.e., unless $\Phi_S^{(+)}(\mathbf{s},t) = i\alpha f_L(t)u_L(\mathbf{s})$.

For this multimode coherent-state field, Eq. (4.3) gives for the probability of difference-number detection

$$P(n_{12};\,\alpha_L,\{\alpha_{jl}\}) = \frac{\exp[-(n_{12} - \eta\{\alpha_L{}^*\alpha + \alpha_L\alpha^*\})^2/2\eta(|\alpha_L|^2 + |\alpha|^2 + \overline{N}_B)]}{[\pi 2\eta(|\alpha_L|^2 + |\alpha|^2 + \overline{N}_B)]^{1/2}}. \quad (4.8)$$

When the LO photon number $|\alpha_L|^2$ dominates the total signal $|\alpha|^2 + \overline{N}_B$, the standard deviation (half-width) of the n_{12} distribution Eq. (4.8) equals $[\eta|\alpha_L|^2]^{1/2}$, that is, the square root of the mean number of photoelectrons generated in both detectors combined. This is the well-known shot-noise level (vacuum, or zero-point, noise) and is intrinsic to the signal coherent state. The n_{12} distribution also clearly shows that the presence of the nonmatched signal $\overline{N}_B$ broadens the difference-number distribution. This is because this part of the signal splits randomly at the beam splitter and so does not subtract exactly on every pulse, giving a further random component to the difference number.

Now consider the case that the signal field is in a (classical-like) statistical mixture of multimode coherent states $|\{\alpha_{jl}\}\rangle$, with probability density $P_S(\{\alpha_{jl}\})$. If we also allow the LO to be in a mixture of coherent-state fields, Eq. (4.3) gives for the difference distribution

$$P(n_{12}) = \int P(n_{12};\,\alpha_L,\{\alpha_{jl}\})P_L(\alpha_L)P_S(\{\alpha_{jl}\}) \times \mathrm{d}^2\alpha_L\mathrm{d}^2\{\alpha_{jl}\}, \quad (4.9)$$

where $P(n_{12};\,\alpha_L,\{\alpha_{jl}\})$ is given by Eq. (4.8). This is a rather general result, encompassing many types of signal, including, for example, most laser outputs and thermal-like light. The nonmatched mean signal $\overline{N}_B$ is assumed here to be constant (i.e., a coherent-state or wideband thermal state), although it could also be considered to fluctuate if another averaging integral is included in Eq. (4.9).

For intrinsically quantum fields, such as squeezed or sub-Poisson light, for which $P_S(\{\alpha_{jl}\})$ is not well defined, one must return to Eq. (4.3). If the LO field is in a coherent state $|\alpha_L\rangle$ (or a mixture of such states) with a photon number much greater than unity and is large enough to dominate the mode-matched signal field but not necessarily the nonmatched signal, then Eq. (4.3) becomes

$$P(n_{12};\,\alpha_L) = \left\langle : \frac{\exp[-(n_{12} - \eta\{\alpha_L{}^*\hat{a} + \alpha_L\hat{a}^\dagger\})^2/2\eta(|\alpha_L|^2 + \overline{N}_B)]}{[\pi 2\eta(|\alpha_L|^2 + \overline{N}_B)]^{1/2}} : \right\rangle_{\mathrm{MMS}}, \quad (4.10)$$

where the quantum expectation is over only the mode-matched signal (MMS) variable $\hat{a}$. Again, $\overline{N}_B$ fluctuations could be averaged over.

5. QUADRATURE DISTRIBUTIONS

Here we use the quadrature-amplitude operator $\hat{x}_\phi = \hat{N}_{12}/|\alpha_L|2^{1/2}$ defined in Eq. (2.17) and define the corresponding real variable $x_\phi = n_{12}/\eta|\alpha_L|2^{1/2}$ (accounting for detector efficiency), where $|\alpha_L|$ is assumed constant. Then we can transform Eq. (4.10) into the probability density $P_\phi(x_\phi;\,\alpha_L)$ for the quadrature amplitude of the mode-matched signal:

$$P_\phi(x_\phi;\,\alpha_L) = \left\langle : \frac{\exp[-(x_\phi - \hat{x}_\phi)^2/2\sigma^2]}{[\pi 2\sigma^2]^{1/2}} : \right\rangle_{\mathrm{MMS}}, \quad (5.1)$$

where $2\sigma^2 = 1/\tilde{\eta}$, in which

$$\tilde{\eta} = \eta\left(1 + \frac{\overline{N}_B}{|\alpha_L|^2}\right)^{-1}. \quad (5.2)$$

In the limit $\overline{N}_B \ll |\alpha_L|^2$, $\tilde{\eta}$ approaches η. Again we see that the nonmatched part $\overline{N}_B$ of the signal broadens the distribution.[53]

Consider the case in which the mode-matched signal is classicallike, i.e., a coherent state $|\alpha\rangle$ or a mixture of such states with (Glauber) distribution $P_S(x,\,y)$, where $\alpha = (x + iy)/2^{1/2}$. Then Eq. (5.1) can be evaluated as

$$P_\phi(x_\phi;\,\alpha_L) = \int \frac{\exp[-(x_\phi - \tilde{x}_\phi)^2/2\sigma^2]}{[\pi 2\sigma^2]^{1/2}} P_S(x,\,y)\mathrm{d}x\mathrm{d}y, \quad (5.3)$$

where $\tilde{x}_\phi(x,\,y) = x\cos\phi + y\sin\phi$. If a single coherent state $|\alpha_c\rangle = |(x_c + iy_c)/2^{1/2}\rangle$ is present, then $P_S(x,\,y) = \delta(x - x_c)\delta(y - y_c)$ and

$$P_\phi(x_\phi;\,\alpha_L) = \frac{\exp[-(x_\phi - x_c\cos\phi - y_c\sin\phi)^2/2\sigma^2]}{[\pi 2\sigma^2]^{1/2}}. \quad (5.4)$$

Note that even with 100% detection efficiency and perfect mode matching, such that $2\sigma^2 = 1$, the quadrature distribution $P_\phi(x_\phi;\,\alpha_L)$ is not a delta function but has half-width σ associated with the shot noise.

One can measure the distributions $P_\phi(x_\phi;\,\alpha_L)$, Eq. (5.1), by repeatedly measuring values of x_ϕ for fixed LO phase ϕ and building a histogram of relative frequencies of the occurrence of each value. This is repeated for various ϕ values.

6. RECONSTRUCTION OF CLASSICAL FIELD STATISTICS

From many measured quadrature distributions, optical homodyne tomography allows one to reconstruct the joint, or Wigner, distribution of both quadrature amplitudes $\hat{x}$ and $\hat{y}$.[5,6,26] We will first write Eq. (5.3) as a marginal (reduced) distribution of an underlying joint distribution $W_S(x,\,y)$. The Glauber distribution $P_S(x,\,y)$ cannot be the joint distribution that we seek, because Eq. (5.3) is not of the form of a marginal (projection) integral. To this end, we define $W_S(x,\,y)$ by the convolution

$$W_S(x,\,y) = \frac{1}{\pi}\int \exp[-(x - x')^2 - (y - y')^2]P_S(x',\,y')\mathrm{d}x'\mathrm{d}y'. \quad (6.1)$$

The distribution $W_S(x,\,y)$ is a smoothed version of $P_S(x,\,y)$. Then it can be shown by integration that Eq. (5.3) can be expressed as

$$P_\phi(x_\phi;\,\alpha_L) = \iint \frac{\exp[-\{x_\phi - \tilde{x}_\phi(x,\,y)\}^2/2\epsilon^2]}{\sqrt{\pi 2\epsilon^2}} \times W_S(x,\,y)\mathrm{d}x\mathrm{d}y, \quad (6.2)$$

where $\tilde{x}_\phi(x, y) = x \cos\phi + y \sin\phi$ as before and $2\epsilon^2 = 2\sigma^2 - 1 = 1/\tilde{\eta} - 1$. In the case that $\tilde{\eta} = 1$, Eq. (6.2) becomes

$$P_\phi(x_\phi) = \iint \delta[x_\phi - \tilde{x}_\phi(x, y)] W_S(x, y) \mathrm{d}x \mathrm{d}y , \qquad (6.3)$$

where the α_L label is dropped because its dependence in Eq. (5.2) is eliminated when $\tilde{\eta} = 1$. When we use $x = x_\phi \cos\phi - y_\phi \sin\phi$ and $y = x_\phi \sin\phi + y_\phi \cos\phi$, this becomes

$$P_\phi(x_\phi) = \int_{-\infty}^{\infty} W_S(x_\phi \cos\phi - y_\phi \sin\phi, x_\phi \sin\phi + y_\phi \cos\phi) \mathrm{d}y_\phi . \qquad (6.4)$$

This integral has the desired form of a marginal distribution, that is, the joint distribution has been summed over the independent random variable y_ϕ to yield the distribution for the other variable x_ϕ.

The integral Eq. (6.4) is also the Radon transform,[54,55] and has the form of a projection of the W_S function onto the x_ϕ axis, as illustrated by the line integrals in Fig. 2. As in Eq. (2.19) the generalized quadratures x_ϕ and y_ϕ are related to x and y by a rotation around the origin of the x–y phase space. As pointed out by Vogel and Risken, Eq. (6.4) can be inverted to yield $W_S(x, y)$, given a set of distributions $P_\phi(x_\phi)$ for all values of ϕ between 0 and π.[26] The formal inversion is

$$W_S(x, y) = \frac{1}{4\pi^2} \int_{-\infty}^{\infty} \mathrm{d}x_\phi \int_{-\infty}^{\infty} \mathrm{d}\xi |\xi| \int_0^{\pi} \mathrm{d}\phi P_\phi(x_\phi) \times \exp[i\xi(x_\phi - x\cos\phi - y\sin\phi)] . \qquad (6.5)$$

In the case that one has measured a sufficient number of distributions $P_\phi(x_\phi)$ for a finite set of discrete ϕ values, the inversion can be carried out numerically by use of the well-studied filtered backprojection transformation familiar in tomographic imaging.[54] If $W_S(x, y)$ does not have structure on a scale finer than the sampling scale, the reconstruction accurately reproduces $W_S(x, y)$.

This idea forms the basis of the method of optical homodyne tomography for measuring the joint distribution $W_S(x, y)$ of quadrature amplitudes for a light mode.

7. RECONSTRUCTION OF QUANTUM-FIELD STATISTICS

In the case of an intrinsically quantum field, i.e., one that does not have a well-defined Glauber distribution, the distribution $W_S(x, y)$ can still be reconstructed by the same experimental method as described above,[5,6,26,27,56] but now it has a different interpretation. In this case it is called the Wigner distribution, which always exists as a well-behaved function, although it may be negative in some regions.[57] It is not, therefore, a true probability distribution but rather a quasi-distribution. It is constructed in a way to preserve uncertainty relation (2.20).[58]

The Wigner distribution for the mode-matched signal field state is defined in terms of the corresponding density operator $\hat{\rho}_S$ as

$$W_S(x, y) = \frac{1}{\pi} \int_{-\infty}^{\infty} \langle x + x' | \hat{\rho}_S | x - x' \rangle \exp(-2iyx') \mathrm{d}x' , \qquad (7.1)$$

where $|x\rangle$ is an eigenstate of the quadrature operator $\hat{x}$. In the case of a pure state there is a one-to-one correspondence between the wave function $\psi(x)$ and the Wigner distribution through the relation $\langle x|\hat{\rho}|x'\rangle = \psi(x)\psi^*(x')$. Generally one can calculate statistical moments of Weyl-ordered quantum-mechanical products of $\hat{x}$ and $\hat{y}$ by evaluating c-number integrals over the Wigner distribution, i.e.,[9,57]

$$\langle (\hat{x}^m \hat{y}^n)_{\mathrm{Weyl}} \rangle = \iint x^m y^n W_S(x, y) \mathrm{d}x \mathrm{d}y . \qquad (7.2)$$

Weyl ordering of $\hat{x}$ and $\hat{y}$ corresponds to symmetric ordering of $\hat{a}$ and $\hat{a}^\dagger$.

It is desired to rewrite Eq. (5.1) for the probability density of quadrature amplitude as an average of some c-number function weighted by the appropriate Wigner distribution. This amounts to converting the average from a normally ordered one in the operators $\hat{a}$ and $\hat{a}^\dagger$ to a symmetrically ordered one. As is shown in Appendix B, in the quantum case Eq. (5.1) can be rewritten precisely in the same form as Eq. (6.2), with $W_S(x, y)$ being given by Eq. (7.1). Then, in the case that $\tilde{\eta} = 1$, Eqs. (6.3) and (6.4) follow also in this case. In fact, the Wigner function is the only function that has the quadrature distributions as its marginals, as in Eq. (6.4). Then the reconstruction Eq. (6.5) uniquely reproduces the quantum Wigner function defined in Eq. (7.1).

How can we say that a well-defined experimental procedure produces both the quantum Wigner distribution and also a classical joint distribution? Actually the function reconstructed is Eq. (7.1), but in the classical limit this function plays the role of a joint distribution: it is positive everywhere and has the correct marginals, Eq. (6.4). In fact, for quasi-classical states having a well-defined distribution $P_S(x, y)$, Eq. (7.1) reduces exactly to Eq. (6.1).[59]

Given the measured Wigner distribution, the density matrix in x representation is easily obtained by an inverse Fourier transform of Eq. (7.1). This procedure has been demonstrated experimentally for squeezed states and for coherent states.[9] In the case of coherent states, which are pure states, the complex wave function for the field state was experimentally obtained, up to an overall arbitrary phase. Other methods have recently been developed for computing the density matrix directly from

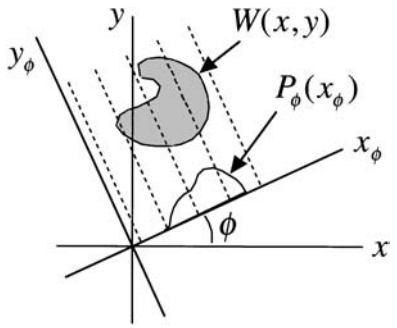

Fig. 2. Generalized amplitudes x_ϕ and y_ϕ are related to quadrature amplitudes x and y by a rotation in phase space. Projection integrals along dashed lines through the Wigner distribution $W(x, y)$ yield the measured distributions $P_\phi(x_\phi)$ for generalized quadrature amplitude x_ϕ. One can reconstruct the Wigner distribution tomographically by measuring $P_\phi(x_\phi)$ for many different rotation angles ϕ, which is equal to the LO phase.

the homodyne data without going through the Wigner function.[60,61]

8. DETECTION INEFFICIENCY

If the effective detector efficiency $\tilde{\eta}$ is less than unity [see Eq. (5.2)], then the just-described reconstruction does not yield the true Wigner distribution of the signal mode, as discussed by Leonhardt and Paul[25,56] and by Kuhn *et al.*[61] To find out what function is reconstructed by the homodyne tomography procedure in this case, we can rewrite Eq. (6.2) as

$$P_\phi(x_\phi) = \int\int \delta[x_\phi - \tilde{x}_\phi(x, y)] W_{\mathrm{Det}}(x, y)\mathrm{d}x\mathrm{d}y\,, \qquad (8.1)$$

where $W_{\mathrm{Det}}(x, y)$ is the (detected) distribution that will be reconstructed by the inverse Radon transform of the data. It can easily be shown by straightforward integration that the following convolution yields the form for $W_{\mathrm{Det}}(x, y)$ that, when put into Eq. (8.1) correctly yields the quadrature distribution in Eq. (6.2):

$$W_{\mathrm{Det}}(x, y) = \frac{1}{\pi 2\epsilon^2} \int\int \exp[-(x - x')^2/2\epsilon^2 - (y - y')^2/2\epsilon^2] W_S(x', y')\mathrm{d}x'\mathrm{d}y'\,. \qquad (8.2)$$

where again $2\epsilon^2 = 1/\tilde{\eta} - 1$. When $\tilde{\eta} = 1$ the smoothing function becomes a delta function and $W_{\mathrm{Det}}(x, y)$ equals $W_S(x, y)$, as before. In general, however, $W_{\mathrm{Det}}(x, y)$ is a smoother function with less detail than $W_S(x, y)$. In principle, the smoothing function could be deconvolved from the measured distribution $W_{\mathrm{Det}}(x, y)$ to yield $W_S(x, y)$, but with experimental data having finite signal-to-noise ratio and systematic errors this is not practical.

9. SPATIAL–TEMPORAL MODE MATCHING

If the signal field is excited in a single spatial–temporal mode $f_S(t)u_S(\mathbf{s})$ different from that of the LO, $f_L(t)u_L(\mathbf{s})$, then a part of it contributes to the detected amplitude α and the remainder to the background $\overline{N}_B$. Express the signal field as

$$\Phi_S^{(+)}(\mathbf{s}, t) = i\alpha_S f_S(t) u_S(\mathbf{s})\,, \qquad (9.1)$$

and note that $f_S(t)u_S(\mathbf{s})$ is not generally orthogonal to $f_L(t)u_L(\mathbf{s})$. Then the detected amplitude is, from Eq. (4.6),

$$\alpha = \eta_{LS}\alpha_S\,, \qquad (9.2)$$

where the complex mode overlap is

$$\eta_{LS}\exp(i\beta) = \int_0^T \mathrm{d}t \int_{\mathrm{Det}} \mathrm{d}^2 s f_L{}^*(t) u_L{}^*(\mathbf{s}) f_S(t) u_S(\mathbf{s})\,, \qquad (9.3)$$

and $0 \le \eta_{LS} \le 1$. Then the non-mode-matched part of the signal (background) is, from Eq. (3.4),

$$\hat{\Phi}_B^{(+)}(\mathbf{s}, t) = i\alpha_B U_B(t, \mathbf{s})\,, \qquad (9.4)$$

where the normalized mode of the background signal is

$$U_B(t, \mathbf{s}) = [1 - \eta_{LS}{}^2]^{1/2}[f_S(t)u_S(\mathbf{s}) - \eta_{LS}\exp(i\beta) f_L(t) u_L(\mathbf{s})] \qquad (9.5)$$

and the background-signal amplitude is

$$\alpha_B = [1 - \eta_{LS}{}^2]^{1/2}\alpha_S\,. \qquad (9.6)$$

This gives for the number of photons in the background signal

$$\overline{N}_B = [1 - \eta_{LS}{}^2]\,|\alpha_S|^2\,. \qquad (9.7)$$

Two conclusions follow: Equation (9.2) shows that the mode-overlap factor η_{LS} acts as an attenuation factor, or effective detector quantum efficiency. This is well known in homodyne detection theory. Equation (9.7) further shows, through Eq. (5.2) or (4.8), that this same factor contributes to the additional broadening of the measured distributions that is due to the non-mode-matched part of the signal.

10. SIMULTANEOUS TIME AND FREQUENCY MEASUREMENT

An important property of the dc-balanced homodyne technique not pointed out previously is that it provides spectral as well as temporal information about the signal field. This arises because if the LO field is frequency tuned [by harmonic variation of the function $f_L(t)$] away from the spectral region of the signal, the integral in Eq. (2.15) that defines the mode-matched amplitude $\hat{a}$ will decrease. To analyze this, define the LO temporal function to be

$$f_L(t) = \exp(-i\omega_L t) h_L(t - t_L)\,, \qquad (10.1)$$

where ω_L is the LO's center frequency and $h_L(t - t_L)$ is a real function with maximum at $t = t_L$. One way to achieve this would be by generating an ultrashort pulse (e.g., 30 fs) and passing it through a tunable bandpass filter, followed by a time-delay optical path. Using the reconstructed joint statistics of quadrature amplitudes, we can determine the mean number of mode-matched signal photons $\overline{N}_{\mathrm{MMS}}(\omega_L, t_L) = \langle \hat{a}^\dagger \hat{a} \rangle$ for a set of ω_L and t_L values. In the semiclassical case, this quantity, for a given LO center frequency ω_L, is equal to

$$\overline{N}_{\mathrm{MMS}}(\omega_L, t_L) = \left\langle \left| \int_0^T \mathrm{d}t\, \exp(i\omega_L t) h_L(t - t_L) \phi^{(+)}(t) \right|^2 \right\rangle, \qquad (10.2)$$

where $\phi^{(+)}(t)$ is the spatial mode-matched signal,

$$\phi^{(+)}(t) = \int_{\mathrm{Det}} \mathrm{d}^2 s u_L{}^*(\mathbf{s}) \Phi_S^{(+)}(\mathbf{s}, t)\,, \qquad (10.3)$$

and the angle brackets indicate an average over multimode coherent-state amplitudes. Equation (10.2) is identical to the general form for time-dependent spectra,[62] with $h_L(t - t_L)$ acting as a time-gate function. For example, it can be put into the same form as that which appears in the time-dependent physical spectrum[63] if we specialize to

$$h_L(t - t_L) = \begin{cases} 0 & t > t_L \\ \exp[\gamma(t - t_L)] & t < t_L \end{cases}. \qquad (10.4)$$

Thus, by scanning the LO center frequency ω_L and arrival time t_L independently, and measuring $\overline{N}_{\mathrm{MMS}}(\omega_L, t_L)$, one obtains both time and frequency information, within the usual time–frequency bandwidth limitations. This method provides an alternative to the nonlinear optical upconversion technique, which has been used to measure

time–frequency information for light emitted by vibrational molecular wave packets.[64]

11. LOCAL-OSCILLATOR FLUCTUATIONS AND HOMODYNE IMBALANCE

In the case of perfect balancing at the beam splitter ($r^2 = t^2$), fluctuations of the LO intensity $I_L = |\alpha_L|^2$ are largely rejected from the n_{12} data.[1,2] To see this, define a relative LO fluctuation by the ratio of the standard deviation to the mean intensity, $f = \Delta I_L/\bar{I}_L$. For a well-designed laser one might have $f = 10^{-2}$ (1% fluctuation). Then it is clear that for $|\alpha|^2 + \bar{N}_B = 0$ (no signal present) the half-width of Eq. (4.8) is $\eta|\alpha_L|^2$, which fluctuates only by 1%, an amount that might be considered negligible.

On the other hand, when signal, imbalance ($r^2 \neq t^2$), or both are present, one needs a more detailed analysis to find the effects of LO fluctuations. Define an imbalance parameter as the difference of the beam splitter's transmissivity and reflectivity, $\delta = t^2 - r^2$, which is assumed to be much less than unity. The total photon number is still given by Eq. (4.4), while the difference number becomes

$$\begin{aligned}\hat{N}_{12} &= \delta(\hat{N}_B - |\alpha_L|^2 + \hat{a}^\dagger\hat{a}) + 2rt(\hat{a}\hat{a}_L{}^\dagger + \hat{a}^\dagger\hat{a}_L) \\ &\cong \delta(\hat{N}_B - I_L) + x_\phi\sqrt{2I_L}\,, \end{aligned} \tag{11.1}$$

where we take the mode-matched signal to be weak and in a coherent state and use $2rt \approx 1$ and Eqs. (2.14) and (2.16). When $\delta = 0$ this reduces to Eq. (2.14).

Consider the difference-number distribution Eq. (4.1) with $P(n_{12}; \alpha_L)$ given by Eq. (4.3). Because I_L fluctuates only a small amount (f), the distribution's intrinsic variance $\eta\bar{N}_T \cong \eta(\bar{I}_L + \bar{N}_B)$ can be approximated as a constant. Again an overbar indicates the mean value. Then the net variance of the distribution Eq. (4.1) is given by

$$\Delta n_{12}{}^2 \cong \eta\bar{N}_T + \eta^2\Delta N_{12}{}^2\,, \tag{11.2}$$

where $\Delta N_{12}{}^2$ is the variance of $\hat{N}_{12}$ defined in relation (11.1). The first term in relation (11.2) is sometimes called the particle noise and the second term the wave noise; if all fields are in coherent states the second term equals zero.

For the variance of the distribution to be within 1%, say, of the shot-noise level ($\Delta n_{12}{}^2 \cong \eta\bar{N}_T$), we need to have

$$\eta\Delta N_{12}{}^2 \leq 10^{-2}\bar{N}_T \cong 10^{-2}(\bar{I}_L + \bar{N}_B)\,. \tag{11.3}$$

The variance $\Delta N_{12}{}^2$ can be estimated under the condition of small f to be

$$\Delta N_{12}{}^2 \cong \delta^2(\Delta N_B{}^2 + \Delta I_L{}^2) + x_\phi\,\frac{\Delta I_L{}^2}{\bar{I}_L}\left(\frac{1}{2}\,x_\phi - \delta\sqrt{2\bar{I}_L}\right), \tag{11.4}$$

assuming that the signal x_ϕ does not fluctuate. We assumed statistical independence of $\hat{N}_B$ with I_L to get the first term here.

In the simple case that there is zero signal ($x_\phi = N_B = 0$), inequality (11.3) implies, assuming that $\eta \approx 1$, that

$$\delta\,\frac{\Delta I_L}{\bar{I}_L} = \delta f \leq (10^{-2}/\bar{I}_L)^{1/2}\,. \tag{11.5}$$

For example, if $\bar{I}_L = 10^6$ photons (typical in experiments[5–9]) and $f = 10^{-2}$, then this condition becomes $\delta \leq 10^{-2}$, meaning that the balancing needs to be within 1%, which is not difficult to achieve. If $f = 0.1$, then we need $\delta \leq 10^{-3}$.

If the mode-matched signal is not zero then the worst case of relation (11.3) occurs when the product $x_\phi\delta$ in relation (11.4) is positive. Then we require the further condition in addition to inequality (11.5):

$$f^2\left(\frac{1}{2}x_\phi{}^2 + |x_\phi\delta|\sqrt{2\bar{I}_L}\right) \leq 10^{-2}\,. \tag{11.6}$$

Using the relation $\bar{N}_{\mathrm{MMS}} \geq (1/2)x_\phi{}^2$ between quadrature amplitude x_ϕ and mode-matched signal photon number $\bar{N}_{\mathrm{MMS}}$, we find two conditions sufficient to guarantee inequality (11.6):

$$f^2\bar{N}_{\mathrm{MMS}} \leq 10^{-2}$$

and simultaneously

$$2f^2|\delta|\sqrt{\bar{N}_{\mathrm{MMS}}\bar{I}_L} \leq 10^{-2}\,. \tag{11.7}$$

For example, if $\bar{I}_L = 10^6$ and $f = 10^{-2}$, then we need $\bar{N}_{\mathrm{MMS}} \leq 100$ and $|\delta| \leq 5 \times 10^{-2}/\sqrt{\bar{N}_{\mathrm{MMS}}} \approx 5 \times 10^{-3}$, which is within the range given above. In summary, in practical systems the number of mode-matched signal photons is limited to approximately 100 or fewer to avoid excess noise introduced by imbalance.

12. CONCLUSIONS

Dc-balanced, pulsed homodyne detection has been shown to have several interesting and unique properties when used as a method for time and frequency resolving the field and intensity statistics of very weak, repetitive optical signals: (1) It detects optical field amplitudes (rather than intensity) in a particular spatial–temporal mode defined by a local-oscillator (LO) pulse. (2) It permits the reconstruction of the joint (Wigner) distribution for the two quadrature-field amplitudes. (3) The statistics can be resolved on a time scale limited only by the duration of the LO pulse, which can be well under 100 fs. (4) The measurement operates at the shot-noise level, allowing mode-matched signals containing less than one photon per pulse to be characterized. (5) The signal can typically contain as many as ~100 mode-matched photons, being limited by practical limits on the degree of dc balancing attainable. (6) Non-mode-matched parts of the signal (spatial or temporal) lead to a broadening of the reconstructed Wigner distribution and so should be kept to a minimum. (7) The detectors used can be photodiodes with quantum efficiency approaching 100%, so quantum statistics of the signal can be obtained without significant degradation caused by detector losses. (8) If losses are present they also lead to a broadening of the reconstructed Wigner distribution. (9) Both time and frequency information about the signal field spectrum can be obtained by scanning the LO center frequency and arrival time independently and measuring the mean signal photon number by the reconstruction method.

An important special case occurs when the signal has a randomly fluctuating phase from pulse to pulse. This occurs, for example, in a pulsed laser that builds up from spontaneous emission[10] or in light strongly scattered in a time-varying random medium.[7] In this case the mean of the mode-matched signal intensity is simply related to the variance of the measured difference number,

$$\overline{N}_{\mathrm{MMS}} = \Delta x_\phi{}^2 - 1/2 = \Delta N_{12}{}^2/2I_L - 1/2\,, \qquad (12.1)$$

independently of the choice of LO phase. This provides a way to observe the mean intensity in nearly real time without invoking the inverse Radon transform to reconstruct the full statistics, which is more time consuming. This idea can be generalized as follows.[10] In the case of random phase it is known[65,66] that the inverse Radon transform simplifies to the Abel inversion formula.[67] This allows one to find explicit formulas to compute the photon-number statistics directly from the quadrature data without invoking the inverse Radon transform. In this case, where the LO is not phase locked to the signal, one loses the ability to characterize the optical phase of the field. This case is discussed in a separate publication.[10]

In the case in which the signal carries phase information relative to a phase-locked LO, such as in pulsed quadrature squeezing,[5,8] the reconstructed Wigner distribution contains full information about the distribution of optical phase.[6,9] This requires that a suitable definition of phase be chosen; it is not unique.[68] On the other hand, it has been pointed out that the Wigner reconstruction is not the most precise way to measure phase distributions.[69] Because the present method is global—it reconstructs distributions of all possible variables—it is not especially precise in determining any particular one, other than the measured quadrature variables.

APPENDIX A

To evaluate the commutator $[\hat{a}, \hat{a}^\dagger]$ by using Eq. (2.15) we need first to evaluate the commutator (at the detector face)

$$[\hat{\Phi}_S^{(+)}(\mathbf{s}, t), \hat{\Phi}_S^{(-)}(\mathbf{s}', t')] = \frac{c}{2\pi D^2} \sum_{j,l} \int_0^\infty \mathrm{d}k_z \times \exp[-i\omega_{jl}(k_z)(t - t')] \times \exp[i\mathbf{k}_{jl} \cdot (\overline{s} - \overline{s}')]\,, \qquad (A1)$$

where we used Eq. (2.5) and Eq. (2.3). In the paraxial approximation the frequencies are given by relation (1.4), and this commutator easily reduces to

$$[\hat{\Phi}_S^{(+)}(\mathbf{s}, t), \hat{\Phi}_S^{(-)}(\mathbf{s}', t')] = \delta(t - t')\delta^2(\mathbf{s} - \mathbf{s}')\,. \qquad (A2)$$

Using this, along with Eq. (2.15) and relation (2.11), gives $[\hat{a}, \hat{a}^\dagger] = 1$. See also Ref. 11.

APPENDIX B

To rewrite Eq. (5.1) for the probability density of the quadrature amplitude as an average of a *c*-number function weighted by a Wigner distribution, as in Eq. (6.2), we can use either of two methods. The first is to write Eq. (5.1) as an integral over the positive-*P* distribution[70] and to use the known relationship between the Wigner distribution and the positive-*P* distribution.[71]

The second method is to make use of the general operator ordering methods developed by Cahill and Glauber.[72] Write Eq. (5.1) as

$$P_\phi(x_\phi) = \mathrm{Tr}[\hat{\rho}\hat{O}], \qquad (B1)$$

where $\hat{\rho}$ is the signal-mode density operator and $\hat{O}$ is the normally ordered operator

$$\hat{O} =: \frac{\exp[-(x_\phi - \hat{x}_\phi)^2/2\sigma^2]}{\sqrt{\pi 2\sigma^2}} : . \qquad (B2)$$

We wish to reexpress Eq. (B1) as

$$P_\phi(x_\phi) = \int_{-\infty}^{\infty} \mathrm{d}x_\phi{}'\mathrm{d}y_\phi{}' W_\phi(x_\phi{}', y_\phi{}') f_{\hat{O}}^{(s)}(x_\phi{}', y_\phi{}')\,, \qquad (B3)$$

where $f_{\hat{O}}^{(s)}(x_\phi{}', y_\phi{}')$ is the *c*-number function associated with $\hat{O}$ in symmetric ordering and $W_\phi(x_\phi{}', y_\phi{}')$ is the signal Wigner function expressed in terms of the generalized quadrature variables defined in the *c*-number equivalent of Eq. (2.19). There is also a *c*-number function associated with $\hat{O}$ in normal ordering, which is

$$f_{\hat{O}}^{(n)}(x_\phi{}', y_\phi{}') = \frac{\exp[-(x_\phi - x_\phi{}')^2/2\sigma^2]}{\sqrt{\pi 2\sigma^2}} \qquad (B4)$$

[and which can be used to evaluate the average Eq. (B1) as an integral with the Glauber–Sudarshan *P* distribution as a weight function]. To obtain the form of $f_{\hat{O}}^{(s)}(x_\phi{}', y_\phi{}')$ we use the general relation between the Fourier transforms of the different associated functions:

$$\tilde{f}_{\hat{O}}^{(s)}(\lambda_\phi, \mu_\phi) = \exp[(\lambda_\phi{}^2 + \mu_\phi{}^2)/4]\tilde{f}_{\hat{O}}^{(n)}(\lambda_\phi, \mu_\phi)\,, \qquad (B5)$$

where the Fourier transforms are defined, for normally or symmetrically ordered functions, as

$$\tilde{f}_{\hat{O}}^{(n,s)}(\lambda_\phi, \mu_\phi) = \int_{-\infty}^{\infty} \mathrm{d}x_\phi{}'\mathrm{d}y_\phi{}' f_{\hat{O}}^{(n,s)}(x_\phi{}', y_\phi{}') \times \exp[i(\lambda_\phi x_\phi + \mu_\phi y_\phi)]. \qquad (B6)$$

Simple calculation then gives for the symmetrically ordered function

$$f_{\hat{O}}^{(s)}(x_\phi{}', y_\phi{}') = \frac{\exp[-(x_\phi - x_\phi{}')^2/(2\sigma^2 - 1)]}{\sqrt{\pi(2\sigma^2 - 1)}}\,. \qquad (B7)$$

Substituting this into Eq. (B3) gives an integral that one can easily convert into the form of Eq. (6.2) by changing variables back to $x = x_\phi{}' \cos\phi - y_\phi{}' \sin\phi$ and $y = x_\phi{}' \sin\phi - y_\phi{}' \cos\phi$.

ACKNOWLEDGMENTS

This research was supported by National Science Foundation grant PHY 9224779.

*Permanent address, JILA, Department of Physics, University of Colorado and the National Institute of Standards and Technology, Boulder, Colorado 80309.

REFERENCES AND NOTES

1. H. P. Yuen and V. W. S. Chan, Opt. Lett. **8,** 177 (1983).
2. G. L. Abbas, V. W. S. Chan, and T. K. Yee, Opt. Lett. **8,** 419 (1983).
3. R. E. Slusher, L. W. Hollberg, B. Yurke, J. C. Mertz, and J. F. Valley, Phys. Rev. Lett. **55,** 2409 (1985); L. A. Wu, H. J. Kimble, J. L. Hall, and H. Wu, Phys. Rev. Lett. **57,** 2520 (1986).
4. R. E. Slusher, P. Grangier, A. LaPorta, B. Yurke, and M. J. Potasek, Phys. Rev. Lett. **59,** 2566 (1987).
5. D. T. Smithey, M. Beck, M. G. Raymer, and A. Faridani, Phys. Rev. Lett. **70,** 1244 (1993).
6. D. T. Smithey, M. Beck, J. Cooper, M. G. Raymer, and A. Faridani, Phys. Scr. **T48,** 35 (1993).
7. M. Beck, M. E. Anderson, and M. G. Raymer, in *Advances in Optical Imaging and Photon Migration*, R. R. Alfano, ed., Vol. 21 of OSA Proceedings Series (Optical Society of America, Washington, D.C., 1994), pp. 257–260.
8. M. E. Anderson, M. Beck, M. G. Raymer, and J. D. Bierlein, Opt. Lett. **20,** 620 (1995).
9. M. Beck, D. T. Smithey, J. Cooper, and M. G. Raymer, Opt. Lett. **18,** 1259 (1993); M. Beck, D. T. Smithey, and M. G. Raymer, Phys. Rev. A **48,** R890, (1993); D. T. Smithey, M. Beck, J. Cooper, and M. G. Raymer, Phys. Rev. A **48,** 3159 (1993).
10. M. Munroe, D. Boggavarapu, M. E. Anderson and M. G. Raymer, "Photon number statistics from phase-averaged quadrature field distribution: theory and ultrafast measurement," Phys. Rev. A (to be published); M. Munroe, D. Boggavarapu, M. E. Anderson, U. Leonhardt, and M. G. Raymer, "High-effiency, ultrafast photon-number statistics from phase-averaged homodyne detection," in *Coherence and Quantum Optics VII*, J. Eberly, L. Mandel, and E. Wolf, eds. (Plenum, New York, to be published).
11. H. P. Yuen and J. H. Shapiro, IEEE Trans. Inf. Theory **IT-24,** 657 (1978).
12. J. H. Shapiro, H. P. Yuen, and J. A. Machado Mata, IEEE Trans. Inf. Theory **IT-25,** 179 (1979).
13. H. P. Yuen and J. H. Shapiro, IEEE Trans. Inf. Theory **IT-26,** 78 (1980).
14. B. Yurke, Phys. Rev. A **32,** 300, 311 (1985).
15. B. Yurke, P. Grangier, R. E. Slusher, and M. J. Potasek, Phys. Rev. A **35,** 3586 (1987).
16. P. D. Drummond, in *Quantum Optics V*, J. D. Harvey and D. F. Walls, eds. (Springer-Verlag, Heidelberg, 1989).
17. K. J. Blow, R. Loudon, S. J. D. Phoenix, and T. J. Shepard, Phys. Rev. A **42,** 4102 (1990).
18. B. Huttner, J. J. Baumberg, J. F. Ryan, and S. M. Barnett, Opt. Commun. **90,** 128 (1992).
19. R. Loudon, in *Coherence, Cooperation and Fluctuations*, F. Haake, L. M. Narducci, and D. F. Walls, eds. (Cambridge U. Press, Cambridge, 1986).
20. B. Yurke and D. Stoler, Phys. Rev. A **36,** 1955 (1987).
21. M. J. Collett, R. Loudon, and C. W. Gardiner, J. Mod. Opt. **34,** 881 (1987).
22. S. L. Braunstein, Phys. Rev. A **42,** 474 (1990).
23. W. Vogel and J. Grabow, Phys. Rev. A **47,** 4227 (1993).
24. W. Vogel and W. Schleich, Rev. A **44,** 7642 (1991).
25. U. Leonhardt and H. Paul, Phys. Rev. A **48,** 4598 (1993).
26. K. Vogel and H. Risken, Phys. Rev. A **40,** 2847 (1989).
27. For a review see M. G. Raymer, D. T. Smithey, M. Beck, M. Anderson, and D. F. McAlister, "Measurement of the Wigner function in quantum optics," in *Proceedings of the Third International Wigner Symposium*, Int. J. Mod. Phys. B (to be published); M. G. Raymer, D. T. Smithey, M. Beck, and J. Cooper, Acta Phys. Polon. **86,** 71 (1994).
28. For a tutorial derivation see Z. Y. Ou and L. Mandel, Am. J. Phys. **57,** 66 (1989).
29. For review and references see U. Leonhardt, Phys. Rev. A **48,** 3265 (1993).
30. These relations are most appropriate in the context of pulsed fields with a local description, as considered here, rather than for monochromatic plane waves, which strictly speaking extend throughout space. See W. Vogel and D.-G. Welsch, *Lectures on Quantum Optics* (Akademie Verlag, **location,** 1994), Sec. 6.3.1; L. Knoll, W. Vogel, and D.-G. Welsch, Phys. Rev. A **36,** 3803 (1987).
31. D. T. Smithey, M. Beck, M. Belsley, and M. G. Raymer, Phys. Rev. Lett. **69,** 2650 (1992).
32. J. Guena, Ph. Jacquier, M. Lintz, L. Pottier, M. A. Bouchiat, and A. Hrisoho, Opt. Commun. **71,** 6 (1989).
33. R. J. Glauber, in *Quantum Optics and Electronics*, C. De Witt, A. Blandin, and C. Cohen-Tannoudji, eds. (Gordon & Breach, New York, 1965), pp. 331–381.
34. P. L. Kelley and W. H. Kleiner, Phys. Rev. **136,** A316 (1964).
35. For discussion see J. H. Shapiro and S. S. Wagner, IEEE J. Quantum Electron. **QE-20,** 803 (1984), App.
36. P. D. Drummond, Phys. Rev. A **35,** 4253 (1987).
37. J. Mostowski and M. G. Raymer, in *Contemporary Nonlinear Optics*, G. P. Agrawal and R. W. Boyd, eds. (Academic, Boston, Mass., 1992), p. 187–234.
38. U. M. Titulaer and R. J. Glauber, Phys. Rev. **145,** 1041 (1966).
39. M. G. Raymer and I. A. Walmsley, in *Progress in Optics*, E. Wolf, ed. (North-Holland, Amsterdam, 1990), Vol. XXVIII, p. 181.
40. Strictly speaking, Eq. (2.10) should contain a sum over all modes, even those that are unexcited. However, because we use Eq. (2.10) only in evaluating normally ordered operator averages, these unexcited modes do not contribute.
41. E. Merzbacher, *Quantum Mechanics* (Wiley, New York, 1970), p. 149.
42. K. W. DeLong, D. N. Fittinghoff, R. Trebino, B. Kohler, and K. Wilson, Opt. Lett. **19,** 2152 (1994).
43. For review see R. Loudon and P. L. Knight, J. Mod. Opt. **34,** 709 (1987).
44. The symbol : : indicates normal ordering of the flux operators at the detectors, i.e., all annihilation operators go to the right of creation operators. Because the transformation Eq. (2.1) does not mix positive- and negative-frequency fields, the normal ordering may be equivalently enforced at the input to the beam splitter.
45. Generally time ordering would also be required, but because the fields are treated as free fields this is irrelevant. See, for example, M. Lax and M. Zwanziger, Phys. Rev. A **7,** 750 (1973).
46. L. Mandel, Proc. Phys. Soc. **72,** 1037 (1958).
47. R. Loudon, *The Quantum Theory of Light* (Oxford U. Press, Oxford, 1983), p. 232.
48. Note that one should not refer to sub-Poisson statistics here because even in the coherent-state case the distribution Eq. (3.3) is not a Poisson.
49. H. M. Nussenvieg, *Introduction to Quantum Optics* (Gordon & Breach, New York, 1974), Chap. 3.
50. P. Meystre and M. Sargent, *Elements of Quantum Optics* (Springer-Verlag, Berlin, 1990).
51. Going from Eq. (3.3) to Eq. (4.1) is an example of the optical equivalence theorem by which any normally ordered expectation value can be replaced by a classical integral if the field state can be described as a mixture of coherent states. See Refs. 49 and 59 below.
52. An alternative, and easier, derivation of Eq. (4.3) is to expand Eq. (3.1) before it is substituted into Eq. (3.2).
53. It has been pointed out that for Eq. (5.1) to be valid it is not clear *a priori* for arbitrary states by how much $|\alpha_L|^2$ needs to exceed the mean signal photon number. See Ref. 22.
54. Herman, G. T., *Image Reconstruction from Projections: The Fundamentals of Computerized Tomography* (Academic, New York, 1980).
55. A computer program for filtered backprojection inverse Radon reconstruction, written by A. Faridani of Oregon State University, is available from M. Raymer.
56. For review see U. Leonhardt and H. Paul, "Measuring the quantum state of light," Prog. Quantum Electron. **19,** 89 (1995).
57. E. P. Wigner, Phys. Rev. **40,** 749 (1932); M. Hillery, R. F. O'Connell, M. O. Scully, and E. P. Wigner, Phys. Rep. **106,** 121 (1984).
58. Single-detector counting distributions have been expressed in terms of Wigner functions in T. Marshall and E. Santos, J. Mod. Opt. **38,** 1463 (1992).

59. One can prove this by using the relation $\hat{\rho}_S = (1/2)\int \mathrm{d}x\mathrm{d}y P_S(x, y)|(x + iy)/\sqrt{2}\rangle\langle(x + iy)/\sqrt{2}|$, a diagonal sum over coherent states. See Ref. 49.
60. G. M. D'Ariano, C. Machiavello, and M. G. A. Paris, Phys. Rev. A **50,** 4298 (1994); H. Paul, U. Leonhardt, and G. M. D'Ariano, Acta Phys. Slovaka **45,** 261; U. Leonhardt, H. Paul, and G. M. D'Ariano, "Tomographic detection of the density matrix," Phys. Rev. A (to be published).
61. H. Kuhn, D.-G. Welsch, and W. Vogel, J. Mod. Opt. **41,** 1607 (1994).
62. K.-H. Brenner and K. Wodkiewicz, Opt. Commun. **43,** 103 (1982).
63. J. H. Eberly and K. Wodkiewicz, J. Opt. Soc. Am. **67,** 1252 (1977); G. Nienhuis, Physica **96C,** 391 (1979); J. Phys. B **16,** 2677 (1983).
64. T. J. Dunn, J. N. Sweetser, I. A. Walmsley, and C. Radzewicz, Phys. Rev. Lett. **70,** 3388 (1993).
65. Z. H. Cho, J. P. Jones, and M. Singh, *Foundations of Medical Imaging* (Wiley, New York, 1993). There is a typographical error in the Abel formula in this source.)
66. U. Leonhardt and I. Jex, J. Phys. A **49,** R1555 (1994).
67. R. Courant and D. Hilbert, *Methods of Mathematical Physics* (Interscience, New York, 1953), Vol. I, Chap. III.
68. See the special issue on Quantum phase: W. P. Schleich and S. M. Barnett, eds., Phys. Scr. **T48,** 5–42 (1993).
69. G. M. D'Ariano, C. Macchiavello, and M. G. A. Paris, Phys. Lett. A **195,** 31 (1994).
70. P. D. Drummond and C. Gardiner, J. Phys. A **13,** 2353 (1980).
71. M. D. Reid and B. Yurke, Phys. Rev. A **46,** 4131 (1992), Eq. (17).
72. K. E. Cahill and R. J. Glauber, Phys. Rev. **177,** 1857, 1882 (1969).